

HetSched: Quality-of-Mission Aware Scheduling for Autonomous Vehicle SoCs

Aporva Amarnath
IBM Research

Yorktown Heights, NY
aporva.amarnath@ibm.com

Subhankar Pal
IBM Research

Yorktown Heights, NY
subhankar.pal@ibm.com

Hiwot Kassa
University of Michigan

Ann Arbor, MI
hiwot@umich.edu

Augusto Vega
IBM Research

Yorktown Heights, NY
ajvega@us.ibm.com

Alper Buyuktosunoglu
IBM Research

Yorktown Heights, NY
alperb@us.ibm.com

Hubertus Franke
IBM Research

Yorktown Heights, NY
frankeh@us.ibm.com

John-David Wellman
IBM Research

Yorktown Heights, NY
wellman@us.ibm.com

Ronald Dreslinski
University of Michigan

Ann Arbor, MI
rdreslin@umich.edu

Pradip Bose
IBM Research

Yorktown Heights, NY
pbose@us.ibm.com

Abstract—Systems-on-Chips (SoCs) that power autonomous vehicles (AVs) must meet stringent performance and safety requirements prior to deployment. With increasing complexity in AV applications, the system needs to meet stringent real-time demands of multiple safety-critical applications simultaneously. A typical AV-SoC is a heterogeneous multiprocessor consisting of accelerators supported by general-purpose cores. Such heterogeneity, while needed for power-performance efficiency, complicates the art of task (process) scheduling.

In this paper, we demonstrate that hardware heterogeneity impacts the scheduler’s effectiveness and that optimizing for only the real-time aspect of applications is not sufficient in AVs. Therefore, a more holistic approach is required — one that considers global *Quality-of-Mission* (QoM) metrics, as defined in the paper. We then propose HetSched, a multi-step scheduler that leverages dynamic runtime information about the underlying heterogeneous hardware platform, along with the applications’ real-time constraints and the task traffic in the system to optimize overall mission performance. HetSched proposes two scheduling policies: MS_{stat} and MS_{dyn} and scheduling optimizations like task pruning, hybrid heterogeneous ranking and rank update. HetSched improves overall mission performance on average by $4.6\times$, $2.6\times$ and $2.6\times$ when compared against CPATH, ADS and 2lvl-EDF (state-of-the-art real-time schedulers built for heterogeneous systems), respectively, and achieves an average of 53.3% higher hardware utilization, while meeting 100% critical deadlines for real-world applications of autonomous driving and aerial vehicles. Furthermore, when used as part of an SoC design space exploration loop, in comparison to the prior schedulers, HetSched reduces the number of processing elements required by an SoC to safely complete AV’s missions by 35% on average while achieving $2.7\times$ lower energy-mission time product.

I. INTRODUCTION

With the growing prominence of fully autonomous vehicles (ground, aerial, surface and underwater), major investments are being made into developing applications to make these vehicles efficient and safe. In order to ensure functionally correct and safe operation, the complexity of state-of-the-art full-stack hardware-software platforms for autonomous vehicles (AVs) has progressively increased over the last decade — specifically in the form of highly-heterogeneous hardware systems driven by highly-heterogeneous software applications.

The resulting “nominal” hardware-software platform for AVs consists of domain-specific systems-on-chips (DSSoCs) with multiple acceleration engines specifically catering to ultra-efficient execution of application kernels for perception, planning, control, and communication. Examples of these platforms include NVIDIA’s DRIVE AGX [7] and Tesla’s Full Self-Driving (FSD) chip [49]. In this context, the existing work focuses mostly on: (i) optimal SoC platforms for AVs to comply with stipulated performance, efficiency and resiliency metrics, and (ii) the development of AV applications that can meet the increasing functionality and safety requirements for autonomy. Little attention has been paid to the aspect of process scheduling for AV applications on heterogeneous DSSoCs. The *de facto* approach relies on schedulers developed for:

- 1) Heterogeneous systems (traditional distributed systems and not SoCs, therefore low variation in execution time across processing elements) [51], [21].
- 2) Real-time constrained applications [3], [4].
- 3) Real-time constrained applications based on the ones listed in 1) above [58], [56], [57].

However, none of these schedulers use dynamic runtime information from the system to efficiently schedule real-time applications on heterogeneous SoCs. Moreover, these schedulers operate in a greedy manner, trying to meet the real-time requirements of individual processes or applications without any consideration of a *global* objective function, defined as the Quality-of-Mission (QoM) metric for AV applications. We define the QoM as a composite metric encompassing both the mission performance, the fraction of mission completed *safely*, *i.e.* while meeting the real-time and safety constraints and the energy consumed.

To demonstrate the value of considering the QoM, we examine the following two schedulers:

- 1) **Quality-of-Mission Agnostic Approach.** The tasks of an AV application, represented as directed-acyclic graphs (DAG), are statically scheduled using the earliest-finish-

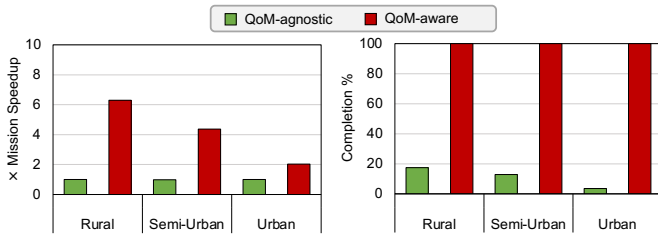


Fig. 1. *Left-axis*: Mission speedup of Quality-of-Mission aware scheduler (*QoM-aware*) over the Quality-of-Mission agnostic scheduler (*QoM-agnostic*) and *Right-axis*: Mission completed by *QoM-agnostic* and *QoM-aware* while operating at the speed achieved by *QoM-aware*, when evaluated under three congestion scenarios: rural, semi-urban and urban.

time and lower-bound approach detailed in [57]. During execution, based on the *safety-criticality level* of a DAG (a specification that indicates how critical the timely execution of a task is for safe AV operation), the tasks are re-ordered to execute on the fastest processing element (PE).

2) **Quality-of-Mission Aware Approach.** Tasks are ranked taking into account the temporal density of safety-critical DAGs in the system, real-time constraints (deadline and criticality-level) along with their heterogeneous execution profiles and dynamic runtime information. This allows the scheduler to make “smarter” scheduling decisions across PEs in highly-heterogeneous SoCs while navigating through dynamic environments, as we propose in this paper.

Figure 1 presents the evaluation of these scheduler variants under progressively more congested navigation conditions (rural, semi-urban and urban). The figure evaluates the schedulers on two metrics: (i) the overall mission time while meeting all real-time constraints and (ii) the percentage of mission completed safely when the AV is operating at the maximum safe speed achievable among the two schedulers. The schedulers are evaluated on a simulated platform with eight general-purpose cores, two GPUs, and one fixed-function hardware accelerator. To complete a *mission* (e.g. safely navigate from a starting location “A” to a destination “B”), the SoC executes a series of *applications*, composed of *tasks* (or kernels or processes). Examples of AV tasks include perception, planning and control.

Figure 1 reveals that scheduling decisions can drastically affect the safe speed of the AV, and consequently its overall mission completion time across varying congestion levels. The *QoM-aware* scheduler outperforms the *QoM-agnostic* scheduler in terms of mission time by 6.3 \times , 4.4 \times and 2.0 \times for the rural, semi-urban and urban scenarios, respectively. Similarly, when *QoM-agnostic* is operated at the safe speed achieved by *QoM-aware*, it is able to complete only up to 17% of the mission before encountering a hazard. This motivates the notion that a holistic approach that is aware of the heterogeneity in hardware and applications along with dynamic run-time information can help make better scheduling decisions even in a highly congested urban-like scenario. Moreover, using this information, the scheduler can stall or prune less-critical applications in favor of more critical ones, or prioritize the execution of a given task on an accelerator

over other tasks which may need to use the same accelerator – the approach followed by *QoM-aware*. The key observation here is that **real-time constrained execution of AV applications without accounting for hardware heterogeneity and dynamic runtime information does not necessarily translate to the best overall mission performance (e.g. mission time).**

In this work, we propose a *QoM-aware* scheduler called HetSched that has been developed as a part of DARPA’s DSSoC program that seeks to develop hardware-software co-design to build efficient DSSoCs. One aspect of the program concentrates on the development of intelligent scheduling for heterogeneous SoCs. HetSched is a multi-level scheduler that leverages the synergy between the underlying heterogeneous hardware platform and the applications’ runtime characteristics to satisfy the growing throughput demand of AVs, while meeting the specified real-time and safety constraints. Specifically, HetSched proposes two scheduling policies: MS_{stat} and MS_{dyn} , in addition to scheduling optimizations, such as *task-traffic reduction*, *hybrid heterogeneous ranking and rank update*. The first step in the operation of HetSched involves profiling the application tasks across *all* the possible PEs in the SoC¹. This information is then used by HetSched to guide its scheduling decisions.

HetSched also uses safety criticality information provided by the application, which is *key* to comply with safety specifications. Runtime information gathered from hardware monitors in the SoC are used by HetSched during operation to keep track of real-time deadlines of the application, and to estimate data movement costs, wait-times of ready tasks, slack available for a DAG, and power consumed by a completed task. These monitors include, but are not limited to, the status of PEs (available/busy), estimated completion time for tasks running on busy PEs, and the execution profile of completed tasks. Moreover, efficient design space exploration of various processing elements (PEs) in the SoC can be achieved by

¹Note that offline application profiling is a common approach across most of the schedulers considered in this work.

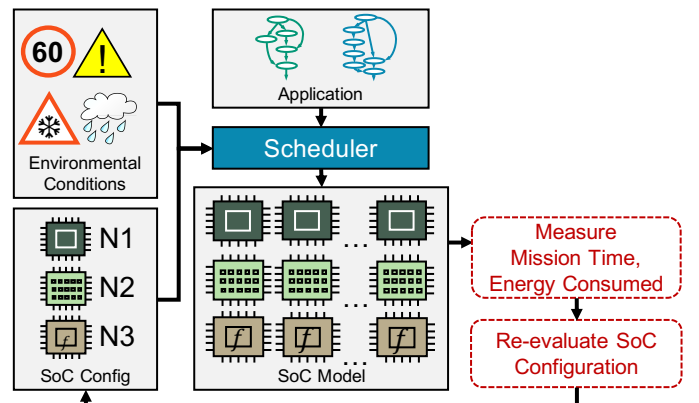


Fig. 2. Use of HetSched to optimize SoC design for AVs while considering QoM metrics. Use of an efficient scheduler in this optimization loop helps reduce the compute requirements of an SoC while improving the mission performance and energy consumption.

using HetSched to optimize for the mission time and energy consumption for AV applications constrained by different environmental conditions as shown in Figure 2.

Specifically, the contributions of this paper are as follows.

- 1) We demonstrate that hardware heterogeneity along with the application’s runtime information is key in determining the scheduler’s effectiveness while unveiling new opportunities for smarter task scheduling.
- 2) We propose HetSched, a multi-level scheduler that follows a holistic approach to optimize the *Quality-of-Mission* (QoM), while meeting real-time safety constraints in autonomous vehicles. The scheduler exploits the highly-heterogeneous nature of the underlying SoC and dynamic run-time information (like maximum/minimum slack available and task wait times) to make better scheduling decisions.
- 3) We introduce optimizations such as *task pruning*, *hybrid-ranking* and *rank update* built upon two HetSched policies (MS_{stat} and MS_{dyn}) that result in a performance improvement of $3.2\times$ (average) for real-world AV applications when compared with state-of-the-art schedulers.
- 4) We show significant reductions in mission time, SoC energy and area using HetSched in a design space exploration (DSE) loop for SoC design. We show that HetSched reduces the accelerator resource requirement of an efficient SoC to safely complete AV missions by 35% (on average), compared to state-of-the-art schedulers [56], [57].

II. BACKGROUND AND MOTIVATION

A. Autonomous Vehicle Applications

To achieve high levels of safety, reliability and precision, AV applications are constituted of highly heterogeneous tasks that can be divided into three types based on their function: *perception*, *planning* and *control* [41]. Through perception tasks, AVs sense the environment and perform obstacle detection, localization and classification to determine further action. Planning tasks are implemented to make decisions in order to achieve the vehicle’s goals such as reaching a destination or searching an unknown location while ensuring safety and mission quality. Lastly, control tasks such as traction control, acceleration, braking, steering, and lane keeping are executed to follow the planned actions. We describe the characteristics of and models for AV applications in the following paragraphs.

1) *Heterogeneity in Execution Time*: Task execution times can vary by orders of magnitude across PEs on a heterogeneous AV SoC [35]. In our experiments, we observed this variation to be up to $300\times$ (Section V). Therefore, to make heterogeneity-aware scheduling decisions, we rely on an offline timing profile for each task that can be stored on-chip along with the application binary. A task’s timing profile comprises both the intra-PE execution cost as well as the inter-PE data movement cost of inputs/outputs for all eligible PEs. The execution cost and the data-movement cost also depend on the number of other tasks in the system and memory contention.

2) *Application Model*: For AVs, all applications and their conforming tasks are fixed at runtime, *i.e.* the addition of a new application (with its offline timing profile) would be provided as a software update to the AV. Based on the type of AV and its mission, these tasks are executed according to a fixed control-flow graph (CFG), where edges in the graph are dynamically decided based on the inputs and decisions made during runtime. We derive directed-acyclic graphs (DAGs) as subgraphs from these CFGs that are statically known, although the arrival and execution of these DAGs are dynamic and determined during vehicle operation. These dynamically arriving static DAGs constitute the input to the scheduler. A DAG contains nodes and edges. We map a task in a CFG to a node in the DAG and dependencies between tasks as edges. Note that a task is an independent unit of work that can execute when its data/control dependencies are resolved. DAGs are generated using compiler techniques for extraction of basic blocks from the CFG.

3) *Safety Criticality Level of Applications*: Depending on the AV’s operating environment, each iteration of the CFG can execute at a different safety-criticality level. For autonomous driving applications, ISO 26262 identifies four Automotive Safety Integrity Levels (ASIL): A, B, C, and D [11]. ASIL-A represents the lowest criticality (*i.e.* operations which can result in no injuries) and D represents the highest criticality (*i.e.* operations that can result in the highest degree of automotive hazard). Similarly, unmanned AV tasks have criticality levels assigned based on the Design Assurance Level (DAL) [12]. For the safe and reliable operation of AVs, it is absolutely necessary to comply with these criticality levels. In this paper, we consider DAGs to belong to two criticality levels:

Non-Critical DAGs: those with criticality 1 ($crit=1$) that arrive periodically to the system. They are equivalent to ASIL A, *e.g.* object recognition on a blind-spot camera while traveling straight on a single-lane road.

Critical DAGs: those with criticality 2 ($crit=2$), that are classified as critical in two ways:

- *Promoted DAGs*: If no $crit=1$ DAG meets its deadline within a time period T_{crit} , then the scheduler can promote it to $crit=2$ in order to provide redundancy and avoid potential hazards in the AV operation, *e.g.* a path-planning operation that uses GPS to calibrate the location of the AV while it is moving along a straight line.
- *Highly-Critical DAGs*: DAGs that represent applications of ASIL levels which can result in a clear safety hazard (B, C, and D) would be $crit=2$ DAGs, *e.g.* forward-camera perception of a stop sign during forward motion.

For safe AV operation, DAGs with $crit=2$ have to be executed within specific *hard deadlines* in order to avoid potential hazards. DAGs with $crit=1$ have *firm deadlines*, *i.e.* if executed within their deadlines they could help improve the mission. Otherwise, the output of the DAG is not useful.

B. Congestion in Environmental Conditions

The safety and resilience of AVs are of prime importance due to the toll they can have on human lives and infras-

structure [37], [55]. Hence, the assessment of AV systems operating in varying dynamic scenarios is crucial [38], [33], [15]. The congestion of an environment is determined by the temporal density of $\text{crit}=2$ DAGs encountered during execution. This can be influenced by conditions like the weather, traffic and terrain. *E.g.* in the case of autonomous driving, the vehicle might encounter several crosswalks while driving from point A to point B in an urban area. In this case, the AV passing each crosswalk could be accompanied by the arrival of a $\text{crit}=2$ DAG. Therefore, the more congested the environment (e.g. more crosswalks), the higher the number of $\text{crit}=2$ DAGs that the AV will have to execute. In this work, we consider three congestion scenarios: *rural*, *semi-urban* and *urban*, however we are not limited by this classification.

C. Application Deadline and Speed of the AV

The AV speed determines the rate at which DAGs arrive at the scheduler. Each DAG is also associated with a *real-time deadline*, determined by the speed of the vehicle (the faster the AV, the tighter the deadline), congestion in the environment and the application criticality. Hence, the AV speed is directly proportional to the rate of DAG arrival and inversely proportional to the deadline. The maximum arrival rate at which the AV meets 100% critical deadlines is considered equivalent to its *maximum safe speed* for a given congestion scenario.

D. Quality-of-Mission (QoM) Metrics

Various figures of merit can be used to measure an AV’s mission quality. In this paper, we use universal metrics that can be applied to all AVs, similar to the ones adopted in [17]. We choose the following QoM metrics to evaluate our scheduler for varying congestion scenarios:

- *Mission time* to complete the objective of the mission, e.g. navigation time from location *A* to location *B*, while complying with safety requirements of meeting deadlines for all DAGs with $\text{crit}=2$.
- *Fraction (or %) of mission completed* at a given speed before missing the first $\text{crit}=2$ DAG deadline. For example, if the best scheduler is able to complete a mission safely while operating at a maximum speed of *S*, then this metric for the scheduler being evaluated is calculated as the % of total critical DAGs of the mission an AV running at speed *S* is able to complete before it fails to meet the deadline of a critical task leading to a hazard.
- *Energy consumed* by the AV SoC for mission completion.

E. Domain-Specific Systems-on-Chips

High heterogeneity in AV applications, real-time constraints, and the demand to process multiple critical applications call for the use of highly heterogeneous systems. These SoC platforms consist of multiple processing elements (PEs) with different performance and efficiency characteristics; namely, CPUs, GPUs, accelerators, *etc.* [49], [8], [6], [59]. Heterogeneous SoCs accelerate the execution of a task by providing increased computational capabilities, reduced data movement

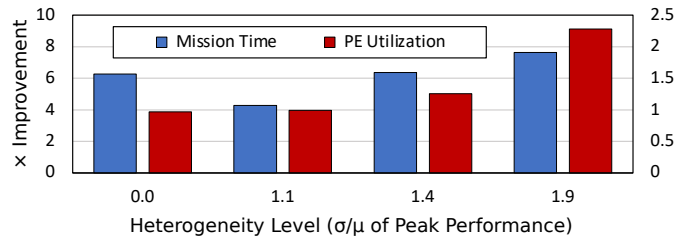


Fig. 3. Effect of SoC heterogeneity, calculated as the coefficient of variation in PE peak performance, on mission speedup and PE utilization of a Quality-of-Mission-aware scheduler (*QoM-aware*) over a Quality-of-Mission agnostic (*QoM-agnostic*). We increase heterogeneity in the system by considering varying number of PEs in the SoC.

cost between PEs, and reduced need to offload computation to cloud servers (or other vehicles, in case of connected vehicle systems [29], [53]), in addition to higher energy efficiency.

The heterogeneity in PEs (Table IV) results in new challenges and opportunities when allocating on-chip resources or making task scheduling decisions. To illustrate the need for global schedulers that are aware of the heterogeneity in an AV SoC, we compare the quality-of-mission agnostic scheduler (*QoM-agnostic*) with the quality-of-mission aware scheduler (*QoM-aware*), as described in Section I, for different hardware configurations. We use the *coefficient of variation* [2] of the PE’s peak performance as a proxy for the heterogeneity level in the SoC. Figure 3 shows that as we increase heterogeneity (by diversifying the PEs), *QoM-aware* is able to improve performance by up to $7.6\times$ over *QoM-agnostic*. By leveraging this heterogeneity information, *QoM-aware* is also able to improve PE utilization by up to $2.2\times$ over *QoM-agnostic*. The takeaway is that synergistic exploitation of the underlying hardware, the application’s real-time requirements (deadline and criticality) and dynamic runtime information can significantly improve mission time and hardware utilization.

F. State-of-the-Art Real-Time and Heterogeneous Schedulers

The processing time of any task comprises of four components: the transfer of input data to the PE that will execute the task (*data movement time*), the time required to make the scheduling decision (*scheduling decision time*), the time spent while the task is waiting to be executed on the scheduled PE (*waiting time*), and the time to execute the task on the scheduled PE (*execution time*). In order to minimize the mission time of an AV, it is critical to reduce all four components. While data movement and execution time are significantly reduced by the use of heterogeneous SoCs, all four components are also highly dependent on the scheduling algorithm. Prior schedulers developed for heterogeneous data-center architectures do help curtail the processing time, but are neither *hetero-aware* (do not efficiently schedule tasks with high-variation in timing profile on an SoC) nor do they optimize for stringent real-time and safety constraints. Furthermore, schedulers developed for real-time-constrained applications are not flexible enough to provide the best QoM metrics or efficiently utilize the underlying hardware. Table I

TABLE I
REAL-TIME AND HETEROGENEOUS SCHEDULERS.

Prior Art	Input	Ranking Type, Parameters	Hetero-Aware	QoM-Aware
CPATH [21]	Single Dynamic DAG	Dynamic Critical path length	×	×
2lvl-EDF[56]	Multiple Static DAGs	Dynamic Earliest deadline first	×	×
ADS [57]	Multiple Static DAGs	Static, Earliest finish time, criticality	×	×
HetSched	Multiple Static DAGs	Dynamic, Deadline, PE variation, criticality	✓	✓

provides a comparison of this work with prior art and briefly discusses them here.

CPATH [21] is a scheduler that prioritizes tasks in the DAG based on a bottom-cost longest-path approach and submits high priority tasks to fast cores and low priority tasks to slow cores with work-stealing enabled. CPATH aims to optimize the response time of a single DAG. When applied to a multi-DAG application with real-time constraints, it fails to meet deadlines at higher arrival rates of DAGs. In contrast, our work targets to meet deadlines in safety-critical multi-DAG scenarios.

2lvl-EDF schedules tasks with the earliest deadline on the earliest finish time PE, as described in [56]. However, it neither considers safety constraints of tasks nor the variation in the timing profile of tasks on the heterogeneous SoC with respect to deadlines.

ADS schedules ranked DAGs based on [51] and dynamically prioritizes tasks with higher criticality levels, as described in [57]. However, ADS neither predicts when to prune non-critical tasks, nor is hetero-aware. HetSched is able to outperform this policy by pruning non-critical tasks, which is further enhanced by HetSched’s hybrid heterogeneous ranking optimization.

None of these prior schedulers operate efficiently on highly-heterogeneous SoCs while optimizing for the real-time requirements of the application and improving overall AV mission performance. Our work targets to fill this void.

III. MISSION- & HETEROGENEITY-AWARE SCHEDULING

HetSched is a multi-level scheduler that exploits the heterogeneous nature of domain-specific SoCs to improve QoM and PE utilization for AV applications. Specifically, HetSched consists of two levels: *Meta-Sched* and *Task-Sched*. *Meta-Sched* translates the mission and application (DAG) level information to tasks, while *Task-Sched* performs the actual task-to-PE assignment and resource management. The two layers communicate using a set of data structures: a *ready queue*, a *completed queue* and a *prune list*.

As depicted in Figure 4, when DAGs arrive for execution, *Meta-Sched* tracks task dependencies, prioritizes ready tasks based on rank, and performs pruning of non-critical tasks. *Task-Sched* receives ready tasks from *Meta-Sched*, updates tasks’ ranks, populates the prune list, assigns tasks to PEs, and sends information of completed tasks to *Meta-Sched*.

TABLE II
DESCRIPTION OF PARAMETERS USED IN HETSCHEd.

Abbreviation	Parameter Description
WCET / BCET/ ACET	Task’s worst/best/avg.-case execution time across all PEs
EET	Task’s estimated execution time
PT	Sum of all WCET of tasks in the path
CPT	Sum of all WCET of tasks in the critical path
CPST	Sum of all WCET of tasks in the segment of the path that intersects the critical path
NCPST	Sum of all WCET of tasks in the segment of the path that does not intersect the critical path
SD / SDR / SR	Task’s sub-deadline / sub-deadline ratio / slack ratio

A. Meta-Sched and Task-Sched Operations

This section describes *Meta-Sched* and *Task-Sched* operation and introduces the various scheduling features in HetSched. Some key terms are defined in Table II.

1) *Dependency Tracking*: *Meta-Sched* processes DAGs to find *ready* tasks. A task is determined as *ready* when all its parent nodes in the DAG have completed execution; *i.e.* it has no incomplete dependencies (incoming edges) in the DAG. Therefore, when a task completes execution on a PE, *Meta-Sched* resolves edges to the children tasks and marks those with no remaining dependencies as *ready*.

2) *Task Prioritization*: Each application (DAG) arriving at *Meta-Sched* has an associated deadline and criticality. Moreover, these DAGs have varying structures in terms of the number of tasks, types of tasks (execution profile) and dependencies (edges). Therefore, to make an informed task scheduling decision (*i.e.* considering the real-time constraints of the DAG and mission performance), *Meta-Sched* assists *Task-Sched* by assigning ranks to ready tasks and ordering them. The rank encodes DAG- and mission-level information as it is determined using the deadline of the parent DAG (the DAG to which the task belongs), criticality and structure, and the task’s execution profile. A task’s *rank* is calculated as:

$$Rank = \frac{Criticality}{Slack}; \quad Eff_Slack = SD - EET \quad (1)$$

where, *Criticality* is the criticality of the task determined by that of the parent DAG, and *Eff_Slack* is the task’s effective slack calculated by *Meta-Sched* as the task’s sub-deadline (*SD*) minus its estimated execution time (*EET*). Therefore, tasks with higher criticality and smaller slack to their deadline are given higher priority. We explore multiple rank assignment policies based on the way *SD* and *EET* are computed. We use the parent DAG’s structure and the task’s execution profile to determine *SD*, *i.e.* for the path within the parent DAG on which the task lies, we find the worst-case execution time (*WCET*) of the path and of the task. The *WCET* of a task is the time required execute the task on the slowest PE. Therefore, by using *WCET* to calculate *SD*, HetSched allows for the tasks to be scheduled on any available PE in the system, whereas using average or best case execution time can bias the scheduler’s decision towards faster PEs. Depending on the way *SD* is calculated, HetSched policies are classified as follows: *MS_{stat}*: In the *MS_{stat}* policy, we determine *SD* as a weighted-ratio of the DAG’s deadline (*Deadline_{DAG}*). This weighted-ratio, called the task’s sub-deadline ratio (*SDR*), is

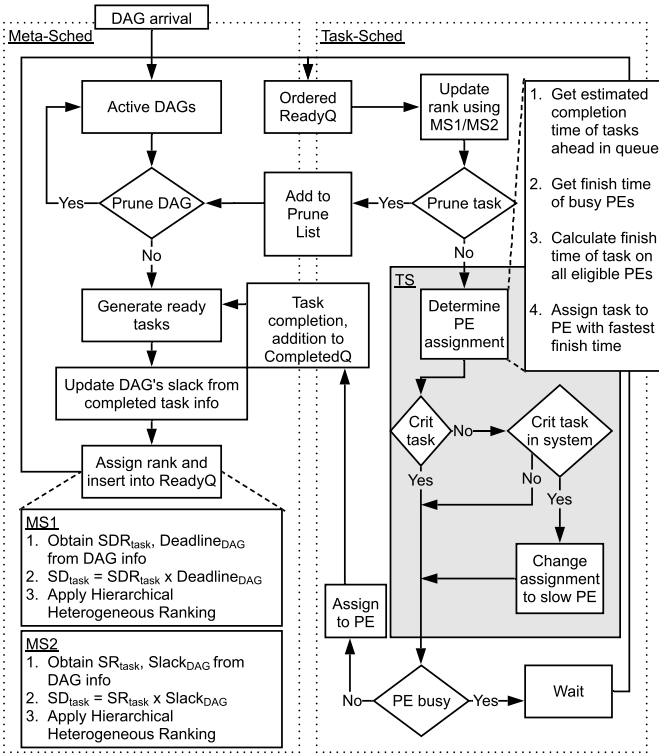


Fig. 4. HetSched operations showing Meta-Sched (mission & DAG processor) and Task-Sched (task scheduler & hardware manager), and their synchronization using the ready and completed queues, and prune list.

calculated as the task's *WCET* relative to its path's execution time. Since each DAG and timing profile of the tasks in it are statically known, *SDRs* can be calculated offline and stored along with the timing profile of the DAG. For a given DAG, the path time (*PT*) is calculated as the sum of the *WCETs* of the tasks in that path. The critical path time (*CPT*) is the one with the largest *PT*. A task's *SDR* and *SD* calculation are based on the path of the DAG on which it lies:

- If the task lies on the critical path or on a path that does not intersect with the critical path, *SDR* is calculated as the ratio of the *WCET* of the task to the path time *PT*:

$$SDR = \frac{WCET}{PT}; \quad SD = SDR \times Deadline_{DAG} \quad (2)$$

- If the task lies on a path which intersects with the critical path, then the path is divided into two segments, the critical path segment (taking a critical-path segment time, *CPST*) and the non-critical path segment (with non-critical-path segment time, *NCPST*). For tasks on the *NCPS*, we first calculate the deadline allocated to the *NCPS*, *Deadline_{NCPS}*, as the *Deadline_{DAG}* minus *Deadline_{CPS}*. Using Equation 2,

$$Deadline_{CPS} = \frac{CPST}{CPT} \times Deadline_{DAG} \quad (3)$$

$$Deadline_{NCPS} = Deadline_{DAG} - Deadline_{CPS} \quad (4)$$

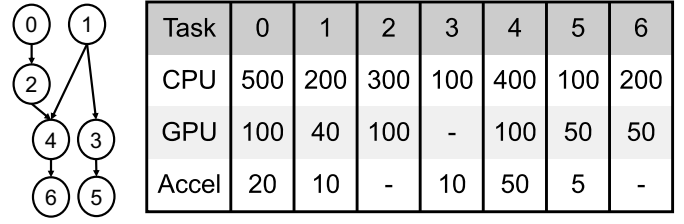


Fig. 5. Left: A 7-task DAG containing three paths: P_0 , P_1 and P_2 . P_0 contains tasks 0, 2, 4 and 6; P_1 contains tasks 1, 4 and 6; and P_2 contains tasks 1, 3 and 5. Right: Timing profile for each task on three types of PEs: CPU, GPU and an accelerator. Using the timing profile, we determine that P_0 is the critical path, P_1 intersects the critical path, and P_2 is independent of it.

For tasks on the *NCPS*, *SDR* and *SD* are calculated similarly, using a path time of *NCPST* and deadline of *Deadline_{NCPS}* as:

$$SDR = \frac{WCET}{NCPST}; \quad SD = SDR \times Deadline_{NCPS} \quad (5)$$

If a given task's sub-deadline *SD* can be calculated using several of the above methods, we pessimistically assign it the smallest of the computed *SD* values. To illustrate with an example, Figure 5 shows a small, 7-task DAG. Let path P_0 , the path consisting of tasks 0, 2, 4 and 6 be the critical path. P_1 contains tasks 1, 4 and 6 and P_2 is composed of tasks 1, 3 and 5. While P_1 intersects the critical path, P_2 does not. Therefore, *SDs* for tasks on P_0 and P_2 , are calculated using Equation 2. Since the *SD* for task 1 on the *NCPS* of P_1 , *SD* can also be calculated using Equation 5, we assign it the lower value of the two.

MS_{dyn}: In this policy, we assign the task's sub-deadline based on a dynamic metric of the DAG. Specifically, *SD* is calculated using the DAG's available slack (*Slack_{DAG}*): the deadline remaining for a DAG during execution, when that ready task's rank is being calculated, as opposed to *MS_{stat}* that uses a static distribution of the DAG's deadline to calculate the task's *SD*. Therefore, *MS_{dyn}* accounts for tasks in the DAG that might have exceeded their sub-deadlines. *MS_{dyn}* adjusts the *SD* of ready tasks based on the available slack of the DAG by calculating a task's *WCET* relative to the execution time of tasks remaining in the task's path:

$$SR = \frac{WCET}{\sum WCET_i}; \quad SD = SR \times Slack_{DAG}. \quad (6)$$

where, *SR* is the task's slack ratio and *WCET_i* is the *WCET* of each remaining task *i* that lies on the same path as the task, including the task itself. If a task lies on multiple paths, then lowest *SR* calculated across all paths is selected. For the DAG in Figure 5, we calculate *SD* and *SR* of the tasks using Equation 6. Since task 1 lies on two paths, P_1 and P_2 , its *SR* is calculated twice and we choose it to be smaller of the two.

Homogeneous Ranking: In this ranking scheme, we calculate *rank_{hom}* as *Crit/Eff_Slack*, where the *Eff_Slack* is determined by using the *WCET* of the task as the *EET* in Equation 1. Therefore, this ranking policy prioritizes critical

tasks that have earlier deadlines over non-critical tasks that have later deadlines.

Heterogeneous Ranking: This ranking approach, $rank_{het}$, improves upon $rank_{hom}$ by accounting for the variation in the execution time of different PEs on the SoC, as well as by adopting contrasting approaches based on the task’s *Crit*. The goal of the scheme is to allow for critical tasks to be prioritized on fast PEs and non-critical tasks to be run on slow PEs without blocking the fast PEs. For this, we first calculate Eff_Slack for each PE type that the task can execute on, as shown in Figure 6 using Equation 1, 2 and 5. We then use the task’s *Crit* and Eff_Slack of each PE type to calculate $rank_{het}$. $rank_{het}$ serves two purposes: (i) prioritization of non-critical tasks that can meet their deadlines on more than one type of PE over those that can meet their deadlines only when executed on a fast PE; and (ii) prioritization of critical tasks with earlier deadlines over those with later deadlines, while considering the PEs that it can execute on.

Hybrid Ranking: To differentiate between tasks of the same $rank_{het}$ in the heterogeneous scheme, we additionally, introduce the scheme of “hybrid ranking” that prioritizes tasks based on both $rank_{hom}$ and $rank_{het}$. However, unlike the homogeneous ranking scheme that uses *WCET* for Eff_Slack to calculate $rank_{hom}$, we assign Eff_Slack based on the PEs that the task can execute on to meet its deadline. This method, shown in Figure 6, is similar to how $rank_{het}$ is determined. Thus, allowing for tasks having the same $rank_{het}$ to be prioritized using $rank_{hom}$ (earliest deadline first). Hybrid ranking also allows for tasks that cannot be executed on all PE types to be prioritized using $rank_{hom}$ and $rank_{het}$ for eligible PE types. Note that this case is not depicted in Figure 6.

3) **Rank Update:** Task-Sched receives ordered ready tasks from Meta-Sched. Before the task assignment, the ranks of the tasks waiting in the ready queue are updated to subtract the time elapsed since previous update from the current effective slack (Eff_Slack). Updating the ready tasks’ ranks can also help in finding non-critical tasks that might not meet their deadline, which can then be considered candidates for pruning, reducing the overall system task traffic. Task-Sched passes these tasks to Meta-Sched for potentially pruning their parent DAGs using the *prune list*.

4) **Task Assignment:** Task-Sched uses a task assignment policy to assign ordered ready tasks in the ready queue to eligible PEs (*i.e.* PEs that can execute it). Furthermore, once a task completes execution, it is pushed into the completed queue along with information about the PE on which it was executed and the timestamp at which it completed execution. We introduce a non-blocking task assignment policy, called TS, that schedules a task in the ready queue to the PE that will result in the earliest estimated finish time for the task, factoring in the execution time of the task, current busy status of the PE and all tasks ahead of this task in the ready queue that are potentially scheduled to the same PE as shown in Figure 4. TS chooses the task to be scheduled using a non-blocking task assignment policy within a window of size w , thus searching w tasks past the head of the queue that could potentially be

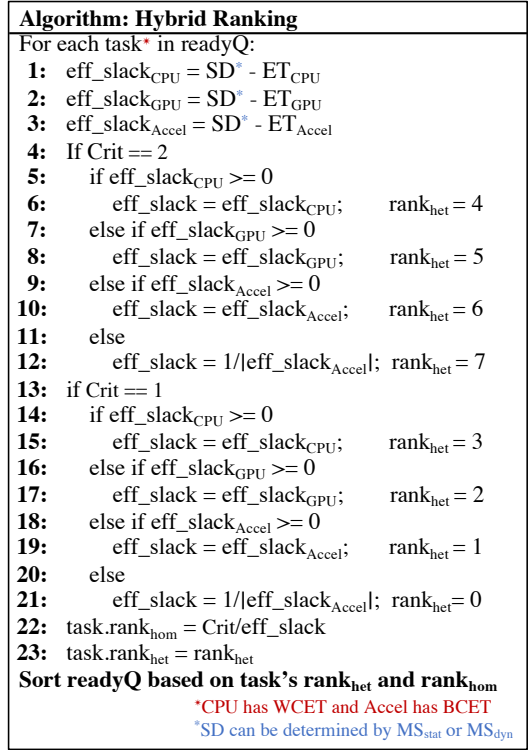


Fig. 6. Algorithm for hybrid ranking of tasks using both $rank_{hom}$ and $rank_{het}$ heuristics.

waiting for the earliest estimated finish time PE to become available. TS is also aware of the timing profile and criticality of each task. Therefore, if the task is non-critical and critical tasks are present in the system, TS can improve utilization by scheduling this task on available slow PEs (Figure 4).

5) **Completed Task Information:** Once a task completes execution, Task-Sched pushes it into the completed queue along with information about the PE on which it was executed and the timestamp at which it completed execution. This information is used by Meta-Sched for dependency tracking and to obtain the data movement cost of children tasks.

6) **Deadline Tracking and Task Pruning:** Meta-Sched can elect to prune DAGs, *i.e.* not execute them at all/any further, thus eliminating non-critical tasks that will not meet their deadlines in order to reduce traffic in the system. After the execution of each task, when Meta-Sched searches the existing DAGs for ready tasks, it also calculates the estimated slack available for each DAG, assuming that ready tasks can execute at their best-case execution time (*BCET*). If the estimated slack available is negative and the DAG has *crit*=1, the entire DAG is pruned. Meta-Sched also prunes DAGs based on the tasks in the prune list, identified during the rank update process. Note that in Algorithm 6, Meta-Sched prunes DAGs that have $rank_type$ 0 or 1, *only if* there are critical DAGs in the system.

B. Summary of Cumulative HetSched Features

In summary, HetSched introduces the following scheduling policies and optimizations.

1) *Task-Sched policy, TS*: A non-blocking scheduler, that schedules ready tasks to the PE with the fastest projected finish time. TS also schedules non-critical tasks to the slowest PEs, if critical tasks are present in the system.

2) *Two-level scheduling policies*: With pruning of non-critical tasks estimated to miss their deadlines. These scheduling policies prioritize ready tasks based on their rank, calculated using the criticality, sub-deadline and estimated execution time of the task, and use TS for their `Task-Sched`.

MS_{stat} determines the sub-deadline of a task statically from the parent DAG’s deadline. MS_{stat} performs best when the deadlines of DAGs are significantly large, *i.e.* when DAGs complete execution with large remaining slack and all tasks are able to complete within their assigned sub-deadlines.

MS_{dyn} uses the task’s parent DAG’s available slack, computed during execution, to dynamically calculate the sub-deadline of the task. Due to this ability to adapt to changes in execution time of tasks, including missing task deadlines, MS_{dyn} performs best for stringent DAG deadlines.

3) *Scheduling optimizations for MS_{stat} and MS_{dyn}* :

Heterogeneous ranking accounts for the variation in execution time of a task on the heterogeneous SoC using dynamic calculation of the rank.

Hybrid ranking uses the effective slack of the tasks along with hetero-ranking to improve overall mission performance by incorporating the state of the system.

Rank Update and Task Pruning revises the task ranks to incorporate time waiting in the ready queue or when critical tasks are encountered. This feature also identifies non-critical tasks that will not meet their deadlines and should be pruned.

IV. EXPERIMENTAL METHODOLOGY

A. Hardware Description

We first profile (offline) a set of AV kernels on an NVIDIA TX1 board, which is representative of an SoC used in real-world AV systems. This information is then used to simulate a heterogeneous SoC with multiple PEs. We assume that the simulated SoC has variants of the Arm Cortex-A57 CPU and the NVIDIA Maxwell GPUs with 256 CUDA cores, and fixed-function accelerators for certain tasks. We consider three systems, named Sys_A , Sys_B and Sys_C , the hardware descriptions of which are shown in Table III. We also consider a unified memory (shared physical address space) between the PEs in the simulated SoC. HetSched, however, is not limited to this specific choice.

B. Application Task Profile

1) *Synthetic Application Tasks*: Our synthetic applications are comprised of three types of tasks: 2D Fast Fourier Transform (fft), 2D convolution (conv) and Viterbi decoding (decoder), taken from the Mini-ERA benchmark suite [5], which simulates a simplified AV with minimal environmental conditions. For fft, we use FFTW3 [27] (CPU) and cuFFT (GPU). For conv, we use Arm Compute Library [1] powered by Neon SIMD extensions (CPU), and cuDNN 5.1 (GPU). We also obtain timing profiles of fft and conv for

TABLE III
SYSTEM DESCRIPTION OF SOC FOR WORKLOAD EVALUATION.

Workload	System	Description
Synthetic	Sys_A	8 single-core Arm Cortex-A57 CPUs 2 NVIDIA Maxwell GPUs 1 CNN/FFT accelerator [19], [45]
Real-World	Sys_B	8 single-core Arm Cortex-A57 CPUs 2 NVIDIA Maxwell GPU 1 tracking accelerator [35] 1 localization accelerator [35] 1 detection accelerator [35]
	Sys_C	N_C^\dagger Single-core Arm Cortex-A57 CPUs N_G^\dagger NVIDIA Maxwell GPUs N_{traA}^\dagger tracking accelerators [35] N_{locA}^\dagger localization accelerators [35] N_{detA}^\dagger detection accelerators [35]

$^\dagger N_C, N_G, N_{traA}, N_{locA}, N_{detA}$ are determined using design space exploration

the accelerators in [19], [45]. Finally, for decoder, we use the GNURadio Viterbi function (CPU) [5] and a PyCUDA implementation [10] (GPU).

2) *Real-World Application Tasks*: We consider two real-world AV benchmarks; ADSuite and MAVBench.

ADSuite [35] provides an autonomous driving application comprised of kernels like object detection (DET), object tracking (TRA), localization (LOC), mission planning and motion planning. For DET, we use YOLOv3 [43], a DNN-based detection algorithm, on a series of 7 images derived from the VOC dataset [25]. We use the Tiny-YOLOv3 pre-trained set of weights, which is much faster and lightweight, but less accurate compared to the regular YOLO model. For TRA, we use GOTURN [30], a DNN-based single object tracking algorithm, on a series of 14 videos in the ALOV++ dataset [47]. For LOC, we use ORB-SLAM [39], a highly-ranked vehicle localization algorithm, on 3 sequences from the KITTI datasets [28]. Further, for our GPU evaluation, we adopt the ORB-SLAM implementation in [9], where the hot paths are rewritten using CUDA. We also obtain timing profile of DET, TRA and LOC on their respective accelerators from [35]. For motion and mission planning, we use the `op_local_planner` and `op_global_planner` [22] kernels in Autoware [34]. The fusion kernel combines the coordinates of the objects being tracked with the AV location. It has a small latency, for which we only consider CPU execution.

MAVBench [17] provides a set of computational kernels that form the building blocks of many aerial vehicle applications. For some of the kernels, we use different algorithms than the ones in [17], in order to better exploit the heterogeneity in our hardware. Specifically, for the perception, tracking and localization kernels, we reuse our ADSuite implementations. For occupancy map generation, we use OctoMap [32] and GPU-Voxels [31] for the CPU and GPU implementations, respectively. OctoMap performs 3D occupancy grid mapping, and GPU-Voxels is a CUDA-based library for robotics planning and monitoring tasks. We generate a map composed of $200 \times 200 \times 200$ voxels. Point cloud generation and collision check consume $10\text{--}1000 \times$ lower latency in comparison to

other kernels (Table I in [17]), and so we only employ CPU implementations for these. For the shortest-path planners, we use the CPU-based parallel RRT (pRRT) [24] implementation in the Open Motion Planning Library (OMPL) [48], on the “Cubicle” benchmark. For the GPU implementation, we use a Poisson-disk samples based GPU algorithm [40]. For frontier exploration, we use the RRT ROS package that implements a multi-robot RRT-based map exploration algorithm [52], on the “single_simulated_house” scenario. Finally, we consider only CPU execution for path tracking as it has a low latency.

We consider two applications from MAVBench in this work, namely Package Delivery, where an aerial AV navigates through an obstacle-filled environment to reach its destination, deliver a package and return back to its origin, and 3D Mapping, that instructs the aerial AV to build a 3D map of an unknown polygonal environment specified by its boundaries.

3) *Data Movement Cost*: To build a realistic evaluation model, we profiled the data movement time across each pair of PE types in the system. We consider the cost for data movement *within* a PE to be zero, *i.e.* if two dependent tasks execute on the same PE, there is no additional overhead. Data movement between a CPU core and a GPU is assumed to be equivalent to the time to flush the parent tasks’ output from the CPU’s caches into main memory, thereby allowing the GPU to load the input data of the child task from the same memory location, since the CPU and GPU share the same physical address space.

The data movement cost from a GPU to a different PE is encapsulated in the timing profile of the task on the GPU. For an accelerator, we consider the data movement cost from/to the accelerator to be the direct-memory access (DMA) transfer cost, since many accelerator designs have their own local memory. We derived empirical data movement cost for the CPU and GPU by profiling the TX1 board, and use DMA transfer rates from published specifications [13] for the accelerators.

4) *Resource Contention*: The execution of a task on a given PE in a realistic SoC is naturally impacted by the volume of parallel tasks executing across the PEs, *i.e.* the contention that the given PE faces due to resources shared with other PEs in the system, such as conflicts at the interconnect network, reduced effective cache capacity if there is no data sharing, *etc.* We used gem5 [16] to simulate a system with $N + 1$ PEs, in order to model the contention due to N PEs. The cache hierarchy and memory are modeled after the TX1 SoC. We constructed an analytical model of the contention cost across the problem sizes used in the evaluated applications, which we used while simulating the benchmarks on HetSched.

C. Energy and Power Model

Power and Energy Estimations. We profiled the average power consumption of each task by measuring the power consumed on the VDD rails of the CPU and GPU of the TX1 board. For the accelerators, we use the estimated power values reported in the prior work (Section IV-A). To compute the end-

to-end energy of the SoC with HetSched, we sum the energy consumed for each task on a PE.

Dynamic Voltage-Frequency Scaling (DVFS). We apply DVFS techniques, similar to those in [42], [14], on the PEs to recuperate low utilization using a fraction of the available slack considering each task’s sub-deadline, which is dependent on the scheduling policy – MS_{stat} or MS_{dyn} (Section III-A). Prior to a task being scheduled onto a PE, the target clock frequency is selected based on: (i) the estimated slack, (ii) the current clock frequency, and (iii) a factor f_{slack} that defines the fraction of slack to be recuperated. Note that naively applying DVFS on the full estimated slack ($f_{slack}=1$) may lead to deadline violations and consequently failure of the mission, *e.g.* if a task T_i , running on a GPU, is slowed down too much, a critical task T_{i+1} , that was formerly waiting on this GPU, could be scheduled onto a slower core. For the purposes of this work, we pessimistically apply a static value for f_{slack} across all DAGs and tasks in a DAG. In the real world, DVFS governors can be integrated within the scheduler to dynamically select f_{slack} per task based on the current PE utilization.

We enable DVFS only for the CPU and GPUs, since we observed that DVFS for even small values of f_{slack} on accelerators leads to low energy savings and mission failures. We use voltage (V_{DD}) and clock frequency (f) points from the embedded DVFS tables in the TX1 to obtain scaling factors for the PE voltage and clock. We further assume the execution time of a task to scale linearly with the PE’s operating frequency, and the power to scale as $V_{DD}^{2.5}$ using DVFS [26].

D. Trace Generation

1) *Synthetic DAG Traces*: In order to evaluate the generality of HetSched, we generate synthetic traces of DAGs arriving at the scheduler that represent applications executed by AVs for varying congestion scenarios. Each entry of the trace consists of the arrival time, type, criticality and deadline of the DAG.

The type of DAG is determined by the composition of the tasks and dependencies between them. We generate different types of DAGs consisting of 5 to 10 tasks of three types of tasks (fft, conv and decoder). A DAG can have a criticality level of 1 or 2, and the fraction of crit=2 DAGs in the trace reflects the congestion in the environment. Each DAG’s deadline is set as the critical path time (CPT). We generate 1,000 DAG traces for the three congestion scenarios (urban, semi-urban and rural) with crit=2 DAG fractions of 50%, 20%, and 10% for urban, semi-urban and rural, respectively. We then evaluate these traces at varying DAG arrival rates (AV speeds) to determine the best QoM metrics.

2) *Real-World Application Traces*: ADSuite and MAVBench have kernel components that make up the end-to-end applications’ CFGs. To generate DAGs, we take the CFGs of both ADSuite and MAVBench and study scenarios that can lead to the execution of different sets of kernels. Such scenarios can arise from the vehicle changing route and leading to the execution of the mission planning

TABLE IV
TIMING AND POWER PROFILE OF EVALUATED KERNELS ON EACH PE-TYPE.

Suite	Task Type	Execution Time			Power (mW)		
		CPU	GPU	ASIC	CPU	GPU	ASIC
Mini-ERA	2D Convolution	583*	349*	180*	634	2225	445
	Viterbi Decoder	1021*	20*	-	864	1228	-
	2D FFT	3193*	97*	4*	1036	6364	4
ADSuite / MAVBench	Object Detection	3531 [†]	156 [†]	96 [†]	3654	467	28
	Object Tracking	1825 [†]	17 [†]	2 [†]	5600	12790	590
	Localization	165 [†]	95 [†]	10 [†]	6133	4457	22
	Mission Planning	1 [†]	-	-	3534	-	-
	Motion Planning	8 [†]	-	-	4222	-	-
ADSuite	Fusion	0.1 [†]	-	-	505	-	-
MAVBench	Occupancy Map Gen + Point Cloud Gen	976 [†]	761 [†]	-	2995	3533	-
	Shortest Path Planner	1005 [†]	379 [†]	-	3302	3533	-
	Collision Check	1 [†]	-	-	500	-	-
	Path Tracking	1 [†]	-	-	501	-	-
	Frontier Exploration	397 [†]	-	-	5980	-	-

*in micro-seconds †in milli-seconds

kernels, and so on. Using the set of kernels executed in the CFG for a particular scenario, we generate DAGs with varying deadlines and criticalities. For ADSuite, as described in [35], we set the deadline of each critical path task to be 100 ms. As no such information is available for MAVBench, each DAG’s deadline is set as the *CPT*. We generate 1,000 DAG traces and choose the same `crit=2` DAG fractions for the three congestion scenarios.

E. Simulation Platform

To explore multiple AV workloads and flexible SoC configurations that are not offered by a fixed real-world system, HetSched is implemented on the STOMP open-source scheduler evaluation platform [54]. STOMP is a queue-based discrete-event simulator used for early-stage evaluation of task scheduling mechanisms in heterogeneous platforms. We augment STOMP to accept DAG-based inputs, while using the underlying queue-based simulator to schedule ready tasks. We also added real-time parameters, such as deadlines and safety criticalities. We realistically model the simulated SoC by providing STOMP with the power and timing profile of tasks obtained from the TX1 platform (Table IV). STOMP also provides the flexibility to add a deviation to the execution time to account for contention on shared resources like memory and buses, which we add as described in Section IV-B4.

V. EVALUATION

We evaluate HetSched for synthetic and real-world traces derived from AV benchmark suites Mini-ERA [5], ADSuite [35] and MAVBench [17]. We also incrementally evaluate our proposed features and compare with state-of-the-art schedulers, namely CPATH [21], ADS [57] and 2lvl-EDF [56] in terms of QoM metrics (Section II-D) and overall PE utilization.

The offline timing profiles generated for key kernels of both the synthetic and real-world applications for representative input data sizes are shown in Table IV.

A. HetSched Optimizations

HetSched introduces two-level schedulers, that use TS as Task-Sched and MS_{stat} and MS_{dyn} along with optimizations for Meta-Sched. We evaluate the optimizations (pruning, hetero-rank ordering and hybrid ranking) to analyze the benefits from each, under varying congestion levels. These features are evaluated with the rank update optimization.

1) *Task Pruning*: Mission time improvement of MS_{stat} and MS_{dyn} along with Pruning over their respective homogeneous ranking based scheduler Hom for different environments is shown in Figure 7. Both MS_{stat} and MS_{dyn} achieve speedups of up to $1.3\times$ over Hom.

2) *Hetero- and Hybrid Ranking*: Employing hetero-ranking (Het) for MS_{stat} and MS_{dyn} helps achieve a reduction in mission time by up to $6.3\times$ and $6.1\times$ for MS_{stat} and MS_{dyn} , as shown in Figure 7. This increased reduction is a combined benefit of Pruning and Het, as hetero-ranking identifies more candidate tasks that can be pruned. Applying the hybrid ranking (Hyb) feature over Het helps to improve mission performance by $2.0\text{--}7.0\times$ for MS_{stat} and MS_{dyn} .

B. Scheduler Evaluation for Real-World Applications

For each of the real-world applications, we compare HetSched against prior baseline schedulers, namely CPATH, ADS and 2lvl-EDF, in terms of QoM metrics and PE utilization. Note that the energy reported here for all systems

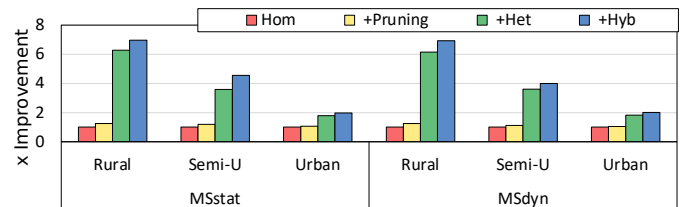


Fig. 7. Improvements in mission time on Sys_A using HetSched with task pruning (Pruning), heterogeneous-ranking (Het) and hybrid-ranking (Hyb) over HetSched with homogeneous-ranking (Hom) for different congestion scenarios.



Fig. 8. Comparison of mission time (left) and energy (right) on Sys_B of HetSched against prior-work schedulers for (a) ADSuite, (b) 3D Mapping, and (c) Package Delivery.

accounts for total power of PEs during task execution and static power when the PE is idle.

1) *Metrics Comparison:* For ADSuite (Figure 8(a)), HetSched enabled with task pruning, hybrid ranking and rank update achieves a 2.1-6.8 \times improvement in mission time for Sys_B over the baseline schedulers. In terms of % mission completed, for Sys_B (not shown), the state-of-the-art schedulers complete just 38%, 5% and 7% of the mission at the maximum safe speed of HetSched for the rural, semi-urban and urban scenarios, respectively, before missing the deadline for a critical DAG. Furthermore, HetSched is able to achieve an average of 2.4 \times better PE utilization over the baselines. This results in the SoC consuming an average of 3.5 \times lower energy when used with HetSched in comparison to the prior schedulers.

HetSched achieves 1.9–5.5 \times improvement in mission time and 1.8–4.0 \times improvement in energy over the state-of-the-art schedulers for 3D Mapping, as shown in Figure 8(b). Additionally, at the maximum safe speed achieved by HetSched, ADS and 2lvl-EDF are each able to complete only a maximum of 9% of the mission before failing for the first critical DAG. Moreover, HetSched achieves up to 1.7 \times better PE utilization. This improvement is lower than that for ADSuite, because Mapping has a high CPU utilization and low accelerator and GPU utilization, since many tasks execute only on the CPU.

The mission time for Package Delivery is shown in Figure 8(c). HetSched achieves 1.9–4.7 \times improvement in mission time and 1.9–2.2 \times improvement in energy over the baseline schedulers. In terms of % mission completion (not shown), ADS achieves a maximum of 38% mission at the maximum safe speed of HetSched for Sys_B . HetSched is able to achieve up to 2.8 \times better average PE utilization for Sys_B .

We note that many of the tasks executed in 3D Mapping and Package Delivery only have CPU implementations (Table IV). As developers implement heterogeneous algorithms for these

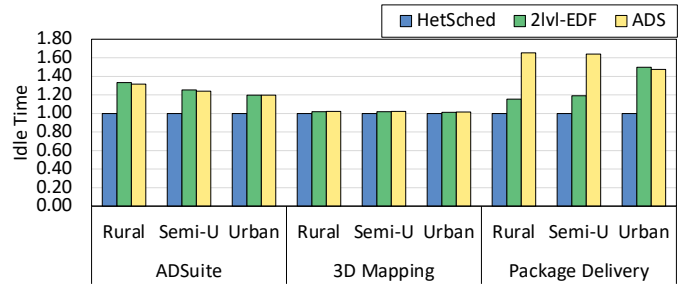


Fig. 9. Idle time on Sys_B using HetSched, 2lvl-EDF and ADS when the system is operating at the speed at which all schedulers complete their mission safely.

tasks, we expect HetSched to show greater benefits in terms of QoM metrics and PE utilization over the baseline schedulers. Moreover, HetSched with MS_{dyn} performs significantly better for ADSuite in comparison to the baseline schedulers, as the deadlines for this application are more stringent (~ 400 ms) in comparison to MAVBench (~ 2000 ms).

2) *Idle Time Comparison:* To provide insight into the gains of HetSched against ADS and 2lvl-EDF, we analyze the efficient use of resources by each scheduler when operated at a speed at which all schedulers can meet deadlines for all $crit=2$ DAGs, i.e. at the speed that the worst scheduler-based system has to operate for safe mission completion. We evaluate the efficiency of resource management by comparing the idle time of all PEs for varying congestion scenarios for each scheduler. Note that we omit the analyses of the CPATH scheduler as the idle time for this scheduler was very small and did not allow for comparison against the real time schedulers.

For ADSuite, HetSched achieves 33% and 32% higher idle time in comparison to 2lvl-EDF and ADS, respectively, for the rural scenario. As the congestion increases, the difference in the idle time between HetSched and 2lvl-EDF and ADS reduces as shown in Figure 9. For 3D mapping, the idle time difference is minimal as the tasks are only run on the CPU and GPU and do not have accelerated tasks implemented yet. For package delivery, as the congestion increases, the idle time decreases for 2lvl-EDF and remains almost same for ADS. HetSched is, therefore, able to increase the speed of the AV and process more tasks per unit time. This increase in idle time can also be used to reduce power consumption of the system if there are external constraints on the speed at which the AV can operate.

3) *Scheduler Overhead:* We also evaluated the overhead of HetSched, i.e. the time spent for dependency tracking, meta information update, task prioritization and task assignment, running on the host Arm processor on the TX1. We observed this overhead to be no more than 19% and 6% of the total mission time for ADSuite and MAVBench, respectively.

4) *Energy and Available Slack:* As discussed in Section IV-C, we adopt a scheme that dynamically recuperates a fraction (f_{slack}) of the slack savings enabled by HetSched on a per-task basis (Section IV-C). Figure 10 (top) shows that our DVFS policy allows HetSched to achieve energy savings of 36%, 22% and 8% for ADSuite, 3D Mapping and Package

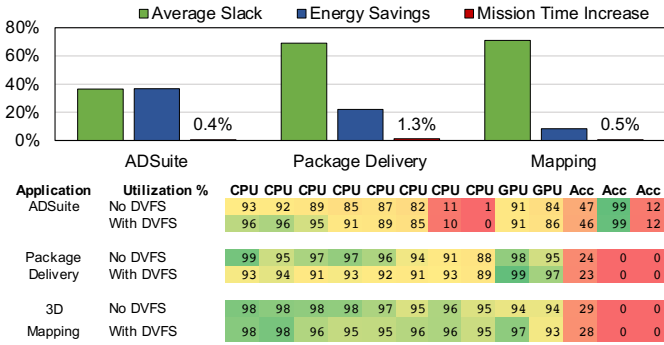


Fig. 10. *Top*. Slack, energy savings and mission overhead for HetSched with DVFS enabled across the three applications. *Bottom*. Per-PE utilization for each application. Results are shown for the rural congestion. The execution run corresponding to the f_{slack} value with best energy savings is reported here. Note that the utilization values for two accelerators (DET and TRA) are zero because the latter two applications do not have any tasks that use these PEs.

Delivery, respectively, while increasing the mission time by just 0.4–1.3%. Note that this is at the maximum safe speed of the AV. At 85% of the AV’s maximum safe speed, we observe energy savings of up to 46.6%, with average PE utilization improvement of up to 18.9% (not shown).

We also show the per-PE utilization with and without DVFS in Figure 10 (bottom), for each of the three applications. Much of the overall energy savings comes from DVFS on the CPU cores, since the CPU is typically the slowest and consumes the most power (Table IV). DVFS improves the utilization of CPUs by 4% on average for ADSuite, yielding the highest energy savings among the applications. DVFS may also reduce the utilization of a subset of the slower cores whenever there are changes to the schedule such that tasks that previously were executed on these PEs now migrate to a faster PE. We observe this for Package Delivery and Mapping, where migration of tasks from CPU to GPU contributes to reduced utilization for the slower CPUs, and yet lowers the overall energy consumption.

5) *SoC Design Optimization*: As described in Section I, having a scheduler-in-the-loop enables design space exploration to determine the best architectural configuration and level-of-heterogeneity for a given AV application. We used HetSched to determine the best SoC configuration that optimizes upon mission time and energy consumption when executing AV applications in the urban scenario. We explore a set of design points, and pick the best SoC configuration as the one with the minimum energy–mission time product and smallest number of PEs (best PE utilization). We present only the results of ADSuite for brevity. The best SoC design configurations, called *SysC*, are (16, 4, 2, 4, 1), (16, 8, 2, 4, 1) and (12, 4, 2, 3, 0) for ADS, 2lvl-EDF and HetSched, respectively, where (A, B, C, D, E) denotes A detection accelerators, B tracking accelerators, C localization accelerators, D GPUs and E CPU cores. As shown in Figure 11, for a reduction in number of PEs by 35%, we are able to achieve an energy-mission time product reduction of $2.7\times$ on average over ADS and 2lvl-EDF when operating in varying congestion levels.

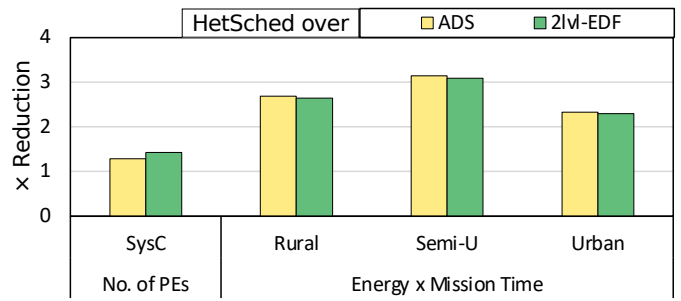


Fig. 11. *Left*: Reduction in number PEs in *SysC* when scheduler-in-the-loop design space exploration is performed. *Right*: Improvement of HetSched in product of energy and mission time for varying congestion levels for ADSuite over prior schedulers for respective *SysC* configurations.

VI. RELATED WORK

AVs pose a challenge with the need to execute heterogeneous applications within stringent real-time and safety constraints. Prior work proposes the use of heterogeneous SoCs to help meet the performance constraints of individual tasks within the heterogeneous applications [35], [49]. However, during runtime, multiple critical applications and tasks are required to be executed simultaneously within their deadlines [23].

A plethora of work exists on scheduling algorithms for heterogeneous systems. Much of the prominent schedulers focus on optimizing the makespan, *i.e.* execution time of a single DAG [51], [20], [21]. Tong *et al.* use Q-learning along with heterogeneous earliest finish time (HEFT) algorithm from [51] to reduce the makespan of a DAG [50]. Shetti *et al.* propose HEFT-NC [46] to optimize ranking and task selection of HEFT [51] by considering global and local processor information. However, as these schedulers are not optimized for the real-time requirements of the AVs and are not built for multiple DAG execution, they would need to be operated on AVs running at very low speeds to meet deadlines for all the critical DAGs of the mission.

To schedule for a multi-DAG scenario on heterogeneous systems, Xu *et al.* develop the reverse HEFT scheduling algorithm [58]. However, this algorithm is not feasible for dynamic systems as it requires *a priori* knowledge of arrival times of all DAGs. Real-time schedulers like earliest deadline first (EDF) and deadline monotonic (DM), in contrast, cater to real-time systems where all tasks have a fixed priority and the criticality of tasks is not considered [23]. However, AVs are categorized as cyber-physical systems and require schedulers that can schedule for mixed criticalities and multiple DAGs [18]. In this regard, Xie *et al.* [57] propose two dynamic schedulers; fairness-based dynamic scheduler (FDS_MIMF) and an adaptive dynamic scheduler (ADS_MIMF), to optimize the makespan of the DAGs and to achieve low deadline miss ratio (DMR) by considering safety and criticality of the system values for high-criticality DAGs, respectively. Wu and Ryu [56], present the best speed fit EDF scheduler that prioritizes tasks according to the earliest deadline and assigns the task to the best possible PE while considering the execution profile of the task, similar to the 2lvl-EDF implementation in

this work. However, none of these work consider that meeting real-time deadlines does not translate to safe completion of mission at the least mission time, *i.e.* while operating the AV at the maximum safe speed. Moreover, use of HEFT-like algorithms for task scheduling on a highly heterogeneous SoC leads to low utilization in slow PEs. HetSched caters to both the requirements of an AV, *i.e.* to meet real-time deadlines for critical DAGs and reduce overall mission time.

Recent work also propose the use of power management systems to help reduce the power and energy consumption of the real-time systems using machine learning techniques [44], [36]. HetSched can work in conjunction with these schedulers to further reduce energy along with the efficient utilization of resources to meet real-time deadlines and power constraints.

ACKNOWLEDGEMENT

This research was developed with funding from the Defense Advanced Research Projects Agency (DARPA). The views, opinions and/or other findings expressed are those of the authors and should not be interpreted as representing the official views or policies of the Department of Defense or the U.S. Government.

VII. CONCLUSION

We presented a multi-level scheduler called HetSched that exploits the highly heterogeneous nature of the underlying domain-specific systems-on-chip (DSSoC) in conjunction with the characteristics of an AV application. HetSched's goal is to improve a global objective function, exemplified by a defined *Quality-of-Mission* (QoM) metric, providing a more *holistic* scheduling approach that looks into the full hardware-software AV stack to improve the overall mission's quality rather than focusing solely on the real-time requirements of individual kernels or applications. Our evaluation shows that HetSched on average improves the mission performance by 2.6–4.6 \times compared to state-of-the-art real-time heterogeneous schedulers. This is achieved with an average of 53.3% higher hardware utilization, while meeting 100% of critical deadlines on real-world AV applications. HetSched can reduce the number of processing elements required in an SoC to safely complete AV missions by 35%, while reducing the energy-mission time product by 2.7 \times , when compared with prior schedulers for AV applications.

REFERENCES

- [1] "The ARM computer vision and machine learning library," <https://github.com/ARM-software/ComputeLibrary>.
- [2] "Coefficient of variation — Wikipedia, the free encyclopedia," https://en.wikipedia.org/w/index.php?title=Coefficient_of_variation.
- [3] "Earliest deadline first scheduling," https://en.wikipedia.org/wiki/Earliest_deadline_first_scheduling.
- [4] "Fixed-priority pre-emptive scheduling," https://en.wikipedia.org/wiki/Fixed-priority_pre-emptive_scheduling.
- [5] "Mini-ERA: Simplified version of the main ERA workload," <https://github.com/IBM/mini-era>.
- [6] "Mobileye: The evolution of EyeQ," <https://www.mobileye.com/our-technology/evolution-eyeq-chip>.
- [7] "NVIDIA Drive AGX platform," <https://developer.nvidia.com/drive>.
- [8] "NVIDIA Orin SoC," <https://nvidianews.nvidia.com/news/nvidia-introduces-drive-agx-orin-advanced-software-defined-platform-for-autonomous-machines>.
- [9] "ORB-SLAM2-GPU." [Online]. Available: <https://github.com/yunchih/ORB-SLAM2-GPU2016-final>
- [10] "Pyterbi: A PyCUDA and PP parallelized Viterbi decoder," <https://github.com/loxodes/pyterbi>.
- [11] "Road vehicles — functional safety," <https://www.iso.org/standard/68383.html>.
- [12] R. F. S. 167, *Software considerations in airborne systems and equipment certification*. RTCA, Incorporated, 1992.
- [13] A. ARM, "Amba axi and ace protocol specification," 2010. [Online]. Available: https://static.docs.arm.com/hi0022/g/hi0022g_amba_axi_protocol_spec.pdf
- [14] H. Aydin, R. Melhem, D. Mossé, and P. Mejía-Alvarez, "Power-aware scheduling for periodic real-time tasks," *IEEE Transactions on Computers*, vol. 53, no. 5, pp. 584–600, 2004.
- [15] S. S. Banerjee, S. Jha, J. Cyriac, Z. T. Kalbarczyk, and R. K. Iyer, "Hands off the wheel in autonomous vehicles?: A systems perspective on over a million miles of field data," in *2018 48th Annual IEEE/IFIP International Conference on Dependable Systems and Networks (DSN)*, 2018, pp. 586–597.
- [16] N. L. Binkert, R. G. Dreslinski, L. R. Hsu, K. T. Lim, A. G. Saidi, and S. K. Reinhardt, "The m5 simulator: Modeling networked systems," *Ieee micro*, vol. 26, no. 4, pp. 52–60, 2006.
- [17] B. Boroujerdian, H. Genc, S. Krishnan, W. Cui, A. Faust, and V. Reddi, "MAVBench: Micro aerial vehicle benchmarking," in *2018 51st Annual IEEE/ACM International Symposium on Microarchitecture (MICRO)*. IEEE, 2018, pp. 894–907.
- [18] E. A. Capota, C. S. Stangaciu, M. V. Micea, and D.-I. Curiac, "Towards mixed criticality task scheduling in cyber physical systems: Challenges and perspectives," *Journal of Systems and Software*, 2019.
- [19] Y.-H. Chen, T. Krishna, J. S. Emer, and V. Sze, "Eyeriss: An energy-efficient reconfigurable accelerator for deep convolutional neural networks," *IEEE journal of solid-state circuits*, vol. 52, no. 1, pp. 127–138, 2016.
- [20] K. Chronaki, A. Rico, R. M. Badia, E. Ayguadé, J. Labarta, and M. Valero, "Criticality-aware dynamic task scheduling for heterogeneous architectures," in *Proceedings of the 29th ACM on International Conference on Supercomputing*, 2015, pp. 329–338.
- [21] K. Chronaki, A. Rico, M. Casas, M. Moretó, R. M. Badia, E. Ayguadé, J. Labarta, and M. Valero, "Task scheduling techniques for asymmetric multi-core systems," *IEEE Transactions on Parallel and Distributed Systems*, vol. 28, no. 7, pp. 2074–2087, 2016.
- [22] H. Darweesh, E. Takeuchi, K. Takeda, Y. Ninomiya, A. Sujiwo, L. Y. Morales, N. Akai, T. Tomizawa, and S. Kato, "Open source integrated planner for autonomous navigation in highly dynamic environments," *Journal of Robotics and Mechatronics*, vol. 29, no. 4, pp. 668–684, 2017.
- [23] R. I. Davis and A. Burns, "A survey of hard real-time scheduling for multiprocessor systems," *ACM Comput. Surv.*, vol. 43, no. 4, Oct. 2011. [Online]. Available: <https://doi-org.proxy.lib.umich.edu/10.1145/1978802.1978814>
- [24] D. Devaurs, T. Siméon, and J. Cortés, "Parallelizing RRT on distributed-memory architectures," in *2011 IEEE International Conference on Robotics and Automation*. IEEE, 2011, pp. 2261–2266.
- [25] M. Everingham, S. M. A. Eslami, L. Van Gool, C. K. I. Williams, J. Winn, and A. Zisserman, "The Pascal visual object classes challenge: A retrospective," *International Journal of Computer Vision*, vol. 111, no. 1, pp. 98–136, Jan. 2015.
- [26] M. Flynn and W. Luk, *Chip Basics: Time, Area, Power, Reliability, and Configurability*, 06 2011, pp. 39–73.
- [27] M. Frigo and S. G. Johnson, "The design and implementation of FFTW3," *Proceedings of the IEEE*, vol. 93, no. 2, pp. 216–231, 2005, special issue on "Program Generation, Optimization, and Platform Adaptation".
- [28] A. Geiger, P. Lenz, C. Stiller, and R. Urtasun, "Vision meets robotics: The KITTI dataset," *The International Journal of Robotics Research*, vol. 32, no. 11, pp. 1231–1237, 2013.
- [29] A. Hashim, T. Saini, H. Bhardwaj, A. Jothi, and A. V. Kumar, "Application of swarm intelligence in autonomous cars for obstacle avoidance," in *Integrated Intelligent Computing, Communication and Security*. Springer, 2019, pp. 393–404.

- [30] D. Held, S. Thrun, and S. Savarese, "Learning to track at 100 fps with deep regression networks," in *European Conference on Computer Vision*. Springer, 2016, pp. 749–765.
- [31] A. Hermann, F. Drews, J. Bauer, S. Klemm, A. Roennau, and R. Dillmann, "Unified GPU voxel collision detection for mobile manipulation planning," in *2014 IEEE/RSJ International Conference on Intelligent Robots and Systems*. IEEE, 2014, pp. 4154–4160.
- [32] A. Hornung, K. M. Wurm, M. Bennewitz, C. Stachniss, and W. Burgard, "OctoMap: An efficient probabilistic 3D mapping framework based on octrees," *Autonomous Robots*, 2013, software available at <http://octomap.github.com>. [Online]. Available: <http://octomap.github.com>
- [33] S. Jha, S. Banerjee, T. Tsai, S. K. S. Hari, M. B. Sullivan, Z. T. Kalbarczyk, S. W. Keckler, and R. K. Iyer, "ML-based fault injection for autonomous vehicles: A case for bayesian fault injection," in *2019 49th Annual IEEE/IFIP International Conference on Dependable Systems and Networks (DSN)*, 2019, pp. 112–124.
- [34] S. Kato, E. Takeuchi, Y. Ishiguro, Y. Ninomiya, K. Takeda, and T. Hamada, "An open approach to autonomous vehicles," *IEEE Micro*, vol. 35, no. 6, pp. 60–68, 2015.
- [35] S.-C. Lin, Y. Zhang, C.-H. Hsu, M. Skach, M. E. Haque, L. Tang, and J. Mars, "The architectural implications of autonomous driving: Constraints and acceleration," in *Proceedings of the Twenty-Third International Conference on Architectural Support for Programming Languages and Operating Systems*, 2018, pp. 751–766.
- [36] S. K. Mandal, G. Bhat, J. R. Doppa, P. P. Pande, and U. Y. Ogras, "An energy-aware online learning framework for resource management in heterogeneous platforms," *ACM Transactions on Design Automation of Electronic Systems (TODAES)*, vol. 25, no. 3, pp. 1–26, 2020.
- [37] P. McCausland, "Self-driving uber car that hit and killed woman did not recognize that pedestrians jaywalk," *Retrieved January*, vol. 29, p. 2020, 2019.
- [38] A. Mehmed, M. Antlinger, and W. Steiner, "The monitor as key architecture element for safe self-driving cars," in *2020 50th Annual IEEE-IFIP International Conference on Dependable Systems and Networks-Supplemental Volume (DSN-S)*, 2020, pp. 9–12.
- [39] R. Mur-Artal, J. M. M. Montiel, and J. D. Tardos, "ORB-SLAM: a versatile and accurate monocular SLAM system," *IEEE transactions on robotics*, vol. 31, no. 5, pp. 1147–1163, 2015.
- [40] C. Park, J. Pan, and D. Manocha, "Realtime GPU-based motion planning for task executions," in *IEEE International Conference on Robotics and Automation Workshop on Combining Task and Motion Planning (May 2013)*. Citeseer, 2013.
- [41] S. D. Pendleton, H. Andersen, X. Du, X. Shen, M. Meghjani, Y. H. Eng, D. Rus, and M. H. Ang, "Perception, planning, control, and coordination for autonomous vehicles," *Machines*, vol. 5, no. 1, p. 6, 2017.
- [42] P. Pillai and K. G. Shin, "Real-time dynamic voltage scaling for low-power embedded operating systems," in *Proceedings of the eighteenth ACM symposium on Operating systems principles*, 2001, pp. 89–102.
- [43] J. Redmon and A. Farhadi, "Yolov3: An incremental improvement," *arXiv preprint arXiv:1804.02767*, 2018.
- [44] A. L. Sartor, A. Krishnakumar, S. E. Arda, U. Y. Ogras, and R. Marculescu, "Hilite: Hierarchical and lightweight imitation learning for power management of embedded socs," *IEEE Computer Architecture Letters*, vol. 19, no. 1, pp. 63–67, 2020.
- [45] M. Seok, D. Jeon, C. Chakrabarti, D. Blaauw, and D. Sylvester, "A 0.27 v 30mhz 17.7 nj/transform 1024-pt complex fft core with super-pipelining," in *2011 IEEE International Solid-State Circuits Conference*. IEEE, 2011, pp. 342–344.
- [46] K. R. Shetti, S. A. Fahmy, and T. Bretschneider, "Optimization of the heft algorithm for a cpu-gpu environment," in *2013 International Conference on Parallel and Distributed Computing, Applications and Technologies*, 2013, pp. 212–218.
- [47] A. W. Smeulders, D. M. Chu, R. Cucchiara, S. Calderara, A. Dehghan, and M. Shah, "Visual tracking: An experimental survey," *IEEE transactions on pattern analysis and machine intelligence*, vol. 36, no. 7, pp. 1442–1468, 2013.
- [48] I. A. Sucan, M. Moll, and L. E. Kavraki, "The open motion planning library," *IEEE Robotics & Automation Magazine*, vol. 19, no. 4, pp. 72–82, 2012.
- [49] E. Talpes, D. Das Sarma, G. Venkataramanan, P. Bannon, B. McGee, B. Floering, A. Jalote, C. Hsiung, S. Arora, A. Gorti, and G. S. Sachdev, "Compute solution for Tesla's full self driving computer," *IEEE Micro*, pp. 1–1, 2020.
- [50] Z. Tong, X. Deng, H. Chen, J. Mei, and H. Liu, "QI-heft: a novel machine learning scheduling scheme base on cloud computing environment," *Neural Computing and Applications*, pp. 1–18, 03 2019.
- [51] H. Topcuoglu, S. Hariri, and M.-y. Wu, "Performance-effective and low-complexity task scheduling for heterogeneous computing," *IEEE transactions on parallel and distributed systems*, vol. 13, no. 3, pp. 260–274, 2002.
- [52] H. Umari and S. Mukhopadhyay, "Autonomous robotic exploration based on multiple rapidly-exploring randomized trees," in *2017 IEEE/RSJ International Conference on Intelligent Robots and Systems (IROS)*. IEEE, 2017, pp. 1396–1402.
- [53] A. Vega, A. Buyuktosunoglu, and P. Bose, "Towards "smarter" vehicles through cloud-backed swarm cognition," in *2018 IEEE Intelligent Vehicles Symposium*, ser. IV 2018, 2018, pp. 1079–1086.
- [54] A. Vega, A. Amarnath, J.-D. Wellman, H. Kassa, S. Pal, H. Franke, A. Buyuktosunoglu, R. Dreslinski, and P. Bose, "STOMP: A tool for evaluation of scheduling policies in heterogeneous multi-processors," *arXiv preprint arXiv:2007.14371*, 2020.
- [55] B. Vlasic and N. E. Boudette, "Self-driving tesla was involved in fatal crash, us says," *New York Times*, vol. 302016, 2016.
- [56] P. Wu and M. Ryu, "Best speed fit edf scheduling for performance asymmetric multiprocessors," *Mathematical Problems in Engineering*, vol. 2017, 2017.
- [57] G. Xie, G. Zeng, Z. Li, R. Li, and K. Li, "Adaptive dynamic scheduling on multifunctional mixed-criticality automotive cyber-physical systems," *IEEE Transactions on Vehicular Technology*, vol. 66, no. 8, pp. 6676–6692, 2017.
- [58] X.-J. Xu, C.-B. Xiao, G.-Z. Tian, and T. Sun, "Hybrid scheduling deadline-constrained multi-DAGs based on reverse HEFT," in *2016 International Conference on Information System and Artificial Intelligence (ISAI)*. IEEE, 2016, pp. 196–202.
- [59] X. Zhang, M. Lok, T. Tong, S. K. Lee, B. Reagen, S. Chaput, P. J. Duhamel, R. J. Wood, D. Brooks, and G. Wei, "A fully integrated battery-powered system-on-chip in 40-nm cmos for closed-loop control of insect-scale pico-aerial vehicle," *IEEE Journal of Solid-State Circuits*, vol. 52, no. 9, pp. 2374–2387, 2017.